AIAA JOURNAL
Vol. 41, No. 5, May 2003

# Toroidal Plasma Thruster for Deep Space Flights

N. N. Gorelenkov* and L. E. Zakharov†
*Princeton University, Princeton, New Jersey 08543*
and
M. V. Gorelenkova‡
*Troitsk Institute for Innovative and Thermonuclear Research, 142092 Troisk, Moscow Region, Russia*

**A conceptual, theoretical assessment of using the toroidal fusion reactor, tokamak, for deep space interplanetary and interstellar missions is presented. Toroidal thermonuclear fusion reactors, such as tokamaks and stellarators, are unique for space propulsion, allowing a design with the magnetic configuration localized inside the toroidal magnetic field coils. Plasma energetic ions, including charged fusion products, can escape such closed configuration at certain conditions as a result of vertical drift in the toroidal rippled magnetic field. Escaping particles can be used for direct propulsion (because toroidal drift is directed one way vertically) or to create and heat externally confined plasma, so that the latter can be used for propulsion. In contrast to other fusion concepts proposed for space propulsion, this concept utilizes the natural drift motion of charged particles out of the closed magnetic field configuration. Also, using deuterium–tritium (D–T) plasma is a novel way to use fusion neutrons with the energy of 14 MeV for direct propulsion ("neutron rocket") for out of solar system missions. A special design of the blanket of the reactor allows neutrons to escape the device in a preferable direction. This provides a direct (partial) conversion of fusion energy into thrust.**

## Nomenclature

| | | |
|---|---|---|
| $a$ | = | minor radius of the plasma |
| $\bar{a}$ | = | averaged acceleration |
| $\boldsymbol{B}$ | = | magnetic field vector |
| $B_{\max}$, $B_{\min}$ | = | maximum and minimum values of the vacuum magnetic field in the toroidal direction |
| $B_R$ | = | component of the magnetic field along $R$ direction |
| $B_Z$ | = | component of the magnetic field along $Z$ direction |
| $B_\theta$ | = | poloidal component of the magnetic field |
| $B_\varphi$ | = | toroidal component of the magnetic field |
| $B_0$ | = | magnetic field at the magnetix axes |
| $\boldsymbol{b}$ | = | unit vector along the magnetic field |
| $F$ | = | thrust |
| $I_{sp}$ | = | specific impulse |
| $I_0$ | = | total plasma current |
| $j_0$ | = | plasma current density |
| $L$ | = | flight distance, km |
| $l$ | = | normalized flight distance |
| $l_{opt}$ | = | normalized time optimized flight distance |
| $M$ | = | spaceship mass |
| $M_L$ | = | mass of the payload |
| $M_w$ | = | mass of the fusion thruster with supporting systems |
| $M'$ | = | mass (and other parameters with prime) in case of constant exhaust velocity |
| $m_D$ | = | deuterium ion mass |
| $N$ | = | number of particles in simulations |
| $N_{\text{coil}}$ | = | number of toroidal field coils |
| $n$ | = | number of "wires" inside the toroidal field coil |
| $n_{\text{pl}}$ | = | plasma density |
| $P$ | = | power of the fusion reactor |
| $P_{\text{loss}}$ | = | thermal fluxes on the first wall |
| $P_z$ | = | space averaged specific (per particle) particle momentum in vertical direction |
| $p$ | = | plasma pressure |
| $p_z$ | = | single fusion particle momentum in vertical direction (flight direction) |
| $q$ | = | magnetic field safety factor $B_\theta r / B_\varphi R$ |
| $R$, $Z$, $\varphi$ | = | cylindrical coordinate system with $\varphi$ is the toroidal angle |
| $R_0$ | = | major radius of the plasma torus |
| $r$ | = | minor radius of a magnetic surface |
| $r_{\text{coil}}$ | = | toroidal field coil radius |
| $T$ | = | temperature of a plasma |
| $t$ | = | time |
| $u$ | = | velocity of the spacecraft, normalized to the minimum exhaust velocity; Eq. (3) |
| $V$ | = | spaceship velocity |
| $V_{\text{orbit}}$ | = | initial velocity of the spaceship at the orbit launch |
| $V_{\text{pl}}$ | = | plasma volume |
| $v$ | = | exhaust velocity |
| $\boldsymbol{v}$ | = | single particle velocity vector in a tokamak |
| $v_{\text{dr}}$ | = | particle drift velocity in the toroidal magnetic field |
| $v_{\alpha 0}$, $v_{n0}$ | = | fusion alpha particle and neutron birth velocities |
| $v_\perp$, $v_\parallel$ | = | particle velocity component perpendicular and parallel to the magnetic field |
| $\alpha$ | = | specific power, power per mass of the thrust producing hardware |
| $\beta$ | = | plasma pressure to magnetic field pressure ratio |
| $\Delta r$ | = | toroidal field coils radial width |
| $\delta$ | = | $(B_{\max} - B_{\min})/(B_{\max} + B_{\min})$ is the magnitude of the magnetic-field ripple |
| $\epsilon$ | = | inversed aspect ratio for a given magnetic surface $\epsilon = r/R_0$ |
| $\epsilon_a$ | = | inversed aspect ratio of a torus $\epsilon = a/R_0$ |
| $\eta$ | = | fraction of generated fusion power used for the thrust |
| $\mu_0$ | = | $4\pi 10^{-7} Hm^{-1}$, permeability in SI units |
| $\rho_L$ | = | particle Larmor radius, $= v_\perp/\omega_c$ |
| $\rho_{L\text{coil}}$ | = | particle Larmor radius in the vicinity of the toroidal field coil |
| $\rho_{L0}$ | = | particle Larmor radius at the magnetic axes |
| $\sigma$ | = | coefficient of proportionality between the rocket and exhaust velocities $\sigma = V/v$ in the case of variable exhaust velocity |

Received 8 November 2001; revision received 22 August 2002; accepted for publication 22 November 2002. 

*Research Physicist, Princeton Plasma Physics Laboratory.
†Principal Research Physicist, Princeton Plasma Physics Laboratory.
‡Leading Engineer, Tokamak Reactor Physics Department.

| | | |
|---|---|---|
| $\tau$ | = | normalized time for the flight; Eq. (3) |
| $\tau_E$ | = | plasma energy confinement time |
| $\psi$ | = | poloidal magnetic flux |
| $\omega_c$ | = | particle cyclotron frequency |

*Subscripts*

| | | |
|---|---|---|
| $a$ | = | plasma edge, last closed magnetic surface at $r = a$ |
| cr | = | critical magnitude of the magnetic field ripple when particles are in the stochastic diffusion regime |
| LFS, HFS | = | low-field side and high-field side of the plasma, respectively |
| max | = | maximum exhaust velocity; birth velocity of fusion products |
| min | = | minimal exhaust velocity |
| pl | = | thermal plasma |
| 0, 1, 2, 3 | = | values at different stages of the mission at $t = 0, 1, 2, 3$ |

## I. Introduction

MAGNETIC fusion reactor configurations were analyzed during the past 40 years and were found to be attractive for space applications, offering unique advantages for space travel to other planets within the solar system and beyond.[1] Among all magnetic fusion concepts, the toroidal reactors, such as tokamaks and stellarators,[2] are unique for fusion space propulsion. They have the lead in magnetic fusion research and allow for a design with the magnetic configuration localized inside the toroidal magnetic field coils, so that the propellant exhaust ions leaving the spaceship will not be affected by the magnetic field. In this paper, the most advanced concept, that is, tokamak, is investigated as a candidate for a fusion thruster for future deep space missions. In addition to having closed magnetic surfaces for a good plasma confinement and for efficient thermonuclear fusion, the tokamak, as we will show, allows for a "vertical" (along the axis of symmetry) drift motion of plasma energetic charged particles out of the system. Trapped in the ripples of the toroidal magnetic field, these particles at certain conditions can escape the reactor through the gaps between the poloidal coils, which are used in tokamaks to create a toroidal field. The same kind of particle loss is present in stellarators.

In contrast to literature emphasizing other fusion concepts proposed for space propulsion, this paper, for the first time, suggests using the natural drift motion of charged particles to extract plasma ions out of the closed magnetic field system. This directed particle flux can be used directly as a propellant. By controlling the regime of the tokamak reactor, the whole range of energies between the plasma ion temperature (20–30 keV in deuterium–tritium plasma and 70 keV in deuterium–$He^3$ plasma) up to the fusion ion energies [3.52 MeV of alpha particles for deuterium–tritium (D–T) fuel at $I_{sp} = 1.3 \times 10^8$ s or 14.7 MeV of protons for deuterium–$He^3$ (D–$He^3$) fuel at $I_{sp} = 5.4 \times 10^8$ s] can be utilized for direct propulsion. This provides control of the exhaust velocity. However, in all practical cases, the flight mission, with the possible exception of interstellar missions, as we will see in Sec. III, requires further enhancement of the thrust. We suggest the use of the energetic particle flux to heat the external plasma confined outside of the closed tokamak toroidal configuration.

Another interesting and novel possibility for extracting momentum from a fusion D–T reactor is to utilize secondary D–T fusion products, neutrons, with the energy of 14.1 MeV. A special design allows neutrons to escape the shield and the blanket of the tokamak. This creates a directed flux of high-energy neutrons with the speed of 52,000 km/s (which is $\frac{1}{6}$ of the speed of the light). As a result, the same tokamak reactor on a spacecraft can potentially cover a wide range of velocities up to 52,000 km/s of propellant particles, which are mostly the byproducts of fusion. This can provide a very efficient direct (and partial) conversion of fusion energy into the directed motion of the propulsion particles. The thrust of such neutron propulsion is rather low and may be used only in interstellar missions.

The tokamak is the most experimentally developed and theoretically understood fusion concept, which many believe is on its way to becoming a commercial fusion power reactor.[2] Recent progress in advanced configurations (for example, low-aspect-ratio compact spherical tokamaks) in new regimes and, most importantly, in increasing the $\beta_{pl}$ parameter up to the level of 40% in volume average, raises hopes of a dramatic reduction in size and weight of the tokamak reactors.[3–5] This raises expectations for the use of advanced tokamak concepts for space propulsion.

Recently, it was proposed that so-called low-aspect-ratio tokamaks, or "spherical tori" (STs), could be used as power generators and sources of plasma.[6–8] However, to make a single particle leave the closed magnetic field configuration with a strong toroidal magnetic field, one must create a poloidal field comparable to the toroidal field, which will require a massive and complex bundle magnetic divertor. Such a divertor may introduce magnetic field perturbation, which limits plasma performance. In this paper, we explore a different idea of breaking particle adiabatic moments in the rippled toroidal magnetic field to move particles out of the magnetic configuration. This seemed to be the key obstacle in allowing tokamaks to be used for direct propulsion. Once outside of the closed magnetic configuration, these byproducts of fusion reactions, energetic ions, can be used for direct thrust or for the heating of externally confined plasma propellant, which has a lower temperature than the plasma temperature of the tokamak. Although fusion research is concentrated around plasma confinement, in this paper we are exploiting the mechanisms of efficient trapped particle losses for creating the thrust, including losses of charged fusion products (for example, $\alpha$ particles and protons) and superthermal tails of the background ion population.

The purpose of this paper is to establish the concept of a tokamak-powered source of fusion thrust and to demonstrate the theoretical feasibility of using a fast fusion product to extract power from the tokamak reactor to create such thrust. The paper is organized as follows: First, we discuss the advantages of using a tokamak-based reactor over other open-field systems in Sec. II. Then, we compare two ways of using fusion propulsion, that is, with a constant and with a variable exhaust velocity, in Sec. III. Different geometries of the toroidal magnetic field are studied in Sec. IV to present the proof of the principle of a tokamak fusion thruster, to explore the ways to optimize the concept by showing the sensitivity of energetic ion extraction to the Larmor radius and other plasma parameters. A summary is given in Sec. V.

## II. Tokamaks vs Other Reactor Concepts

Though many toroidal systems, such as tokamaks and stellarators, may fit into the fusion thruster concept that we are proposing, we focus on the tokamak reactor as a base of the concept and investigate it in detail. Simply put, the tokamak is represented by a strong toroidal magnetic field created by the poloidal coils. The toroidal magnetic field confines the plasma. A single particle in such a field moves along the magnetic-field lines and performs the gyro motion perpendicular to the magnetic-field direction. To compensate for the perpendicular toroidal magnetic ambipolar drift of the gyro orbit, an electric current needs to be generated in the plasma. A toroidal current creates a rotational transform for the particle longitudinal motion so that both electrons and ions are confined. (See Ref. 2 for more details.) Note that in stellarators, rotational transform is created by the external coils.

Even though the tokamak is the most advanced reactor concept, its closed magnetic field lines are thought to be unsuitable for direct thrust. This is because there is no escape path for the plasma out of the reactor, and, to create one, a massive poloidal diverter has to be employed.[8] This would complicate the whole system. Instead, the open-field line configurations such as magnetic dipoles,[9] adiabatic traps, or mirror machines are considered attractive for fusion propulsion, as are field-reversed configurations.[1]

For example, the magnetic configuration of the mirror machines (behind the mirror point) looks very similar to the nozzle of the jet engine and seems to be ideal for utilizing the parallel motion of the plasma particles escaping into the loss cone for propulsion. There

are open questions currently under investigation that are common to all of the fusion thrusters, such as the problem of plasma detachment. Plasma detachment means that plasma that left the system may come back along the magnetic-field lines to another end of the trap. A special design for the nozzle may be required to solve this problem and is currently under research[10] (also, private communication with S. A. Cohen).

The magnetic field is localized inside the toroidal field coils in a tokamak design. Only energetic particles can escape in such a configuration, whereas the fuel is left in the plasma to contribute to the burning. Thus, if the energetic particle escapes the toroidal field due to the drift motion, there are no obstacles for it to leave the spacecraft. With a statistically preferable direction of motion of such particles, this creates the propulsion momentum for the spacecraft with a high $I_{sp}$. To further enhance the thrust and lower the $I_{sp}$ (by increasing mass throughout) one could trap escaping fusion products in a magnetic container to heat a working propellant. This is similar to the design of the proposed antiproton propulsion system[11] and other fusion reactor propulsion systems.[1,9] As we will show, at a fixed power of the generator, the thrust is inversly proportional to the exhaust velocity of the propellant, so that at least at the initial stage of the flight, one would need such an external plasma to enhance the spaceship thrust. The magnetic container, similar in shape to a mirror machine to provide finite confinement of the extermal plasma, should be attached to the tokamak, which will allow the capture of fusion products. Plasma in such an external container will be isolated from the plasma inside the tokamak reactor if its magnetic field is much smaller than the magnetic field of the tokamak itself. On the other hand, the magnetic field of the container should be strong enough for alpha particles to be magnetized so that they would transfer their energy to the plasmsa inside this container. The other open end of such a container will serve as a nozzle to let the plasma escape and to control the specific impulse. The specific design of the rocket at this stage is beyond the scope of this paper. To make estimates of our design performance in the next section, we adopt the major technical features of a tokamak-based rocket from Ref. 7.

Adiabatic magnetic traps or mirror machines initially attracted a lot of attention as candidates for the fusion reactor, but were proven to have a very low-energy confinement time, which is critical for building the self-sustained burning plasma reactor. Kinetic instabilities in earlier experiments, such as that driven by the loss cone in the velocity space, prevented the plasma from achieving high-energy confinement times because achievable trapping magnetic fields are not strong enough to shrink the loss cone and achieve the required confinement. Recently, experiments on mirror machines, such as gasdynamic traps[12] and the tandem mirror GAMMA 10 (Ref. 13) devices, showed that better stability and confinement properties of the plasma are achievable. However, the confinement time is still at least an order of magnitude lower than that in tokamaks, which places mirror machines behind tokamaks in the development of practical terrestrial fusion reactors. More complex geometries[14] suffer from the same problems.

On the other hand, tokamaks have been around for a few decades. They are extensively studied and are on the verge of being built as demo reactors.[15] Experimentally, they have already achieved conditions in which the power used for plasma heating almost equals the power released during the plasma discharge.[16] New concepts with high plasma beta and low machine size emerged recently. One of these concepts is known as a spherical tokamak and was studied in the United States and the United Kingdom with a record volume-average achievable beta $\beta_{pl} \simeq 40\%$, with local beta approaching unity. (See Refs. 3–5 and references therein.)

Our proposal of the tokamak-powered rocket combines the most advanced fusion concept with direct plasma thrust, making this a very attractive approach for deep space vehicles requiring high-power propulsion systems.

## III. Requirements for the Propellant and Thruster Performance

In this section, we prove that, for more practical missions, such as missions within the solar system, there is a need for external plasma in which the fusion power carried by charged products is transformed in to the propellant. We also show examples of the performance of the fusion, tokamak-based thruster. This is demonstrated in two ways, using variable and constant propellant exhaust velocity (specific impulse). In the first approach, we vary the propellant exhaust velocity depending on the rocket speed, whereas in the second, only fusion products are used as propellants with exhaust velocity equal to their birth velocity. The big advantage of using the controllable propellant velocity is that it allows for control of the thrust.

For simplicity, we assume that all propellant particles are leaving the rocket with the same velocity. This allows us to solve the problem analytically, whereas, for practical purposes, one should use some averaged velocity of the propellant, or a specific impulse (because the propellant has a velocity distribution), and solve the system of differential equations numerically. In the first scenario, the variable exhaust velocity (VEV) evolution is prescribed according to $v = V/\sigma$, $\sigma = \text{const} < 1$. There is extensive literature on the problem of variable and constant exhaust velocity rocket equations, such as, for example, Refs. 17–19. For the problem we formulated, we obtained one particular analytical solution with a new time dependence of the spaceship mass determined by the modified rocket equation:

$$M(t) \simeq M_0[V_0/V(t)]^{\sigma} \tag{1}$$

(Appendix), connecting the spaceship mass at a given $t$ with its mass at takeoff time, $t = 0$. Also, as we will show later in this section, the VEV analytical solution can demostrate how to optimize the system. In the second case, constant exhaust velocity (CEV), which obeys the conventional rocket equation [Appendix, Eq. (A2)], we prescribe the exhaust velocity to be equal to the fusion product birth velocity. In this case, no external plasma is needed.

The tokamak-based generator producing $P$ gigawatts of power is considered. [Note that the planned International Thermonuclear Experimental Reactor (ITER) prototype of the tokamak reactor is designed for $P \simeq 1$ GW (Ref. 15).] We also assume that the power is directly transformed into the thrust with the efficiency $\eta < 1$, which gives the fraction of power utilized for heating the propellant. The amount of thrust produced by the propellant can be easily expressed in terms of generated power:

$$F = 2\eta P/v \tag{2}$$

From this equation, one can see that VEV offers more flexibility to optimize the use of generated power: The lower the $v$, the higher the thrust. Depending on the mission, it may be required for space flight to minimize the ratio $M_0/M > 1$ and/or flight time. We will assume hereafter that, at the destination, the mass of the rocket consists of the fusion thruster with supporting systems and the payload $M \equiv M_w(1 + M_L/M_w)$.

In the VEV case, from Eq. (1), it can be seen that one needs finite initial velocity $V_0$ to have finite $M_0$. Therefore, a CEV scheme with a small $v$ may be needed before VEV. This also follows from the requirements that the externally confined plasma propellant may have some minimum velocity $v_{\min}$, required for good confinement. At this stage, the thrust is at a maximum [Eq. (2)] and spaceship velocity is bounded by inequalities $V_{\text{orbit}} \le V < v_{\min}\sigma$, where $V_{\text{orbit}}$ is its velocity on the Earth orbit. It is convenient to introduce dimensionless time and rocket velocity:

$$\tau = \frac{2\eta P t}{v_{\min}^2 M_0} = \frac{2\alpha t}{v_{\min}^2(1 + M_L/M_w)}\frac{M}{M_0}, \qquad u = \frac{V}{v_{\min}} \tag{3}$$

In the Appendix, expressions for CEV and VEV are obtained. Figures 1 and 2 give a comparison of the overall performance of CEV and VEV scenarios. In Fig. 1, shown are the normalized flight distance $l$ as a dotted line and mass ratio $M/M_0$ for VEV as dashed curve, time optimized distance from Ref. 17 as circular points, CEV distance $l'$ as solid line and its mass ratio $M'/M_0$ as dotted line with points vs normalized time. Shown also is the real time of the flight for chosen normalization constant (discussed later) as a function of $\tau$.

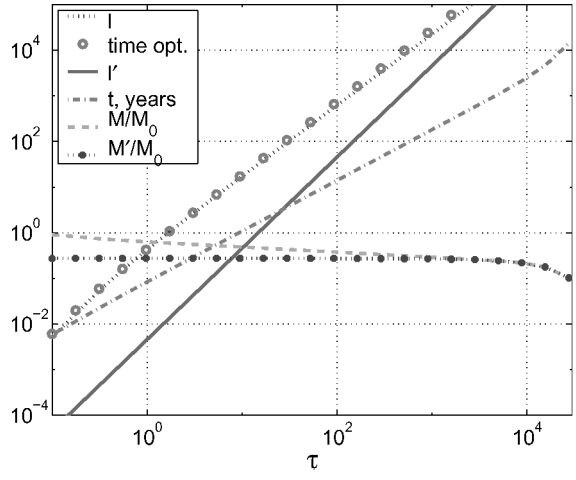


**Fig. 1 Comparison of the performance of the conventional rocket equation solution, CEV [Eq. (A11)], with the VEV solution [Eq. (A9)] at $\sigma = \frac{1}{5}$, where the stages are separated by times $\tau_1 = 0.18$, $\tau_2 = 362$, and $\tau_3 = 9.6\tau_2$.**

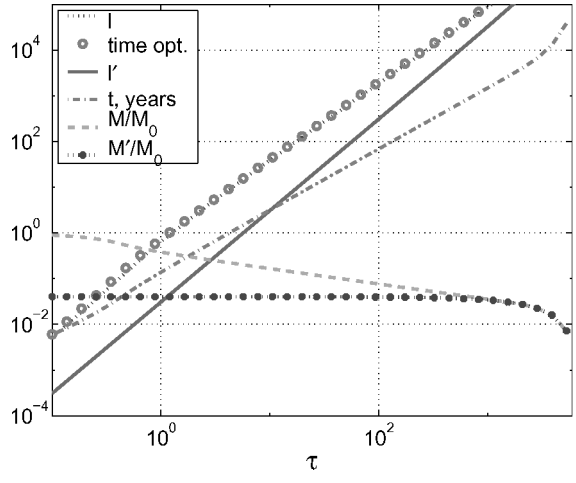


**Fig. 2 Same as in Fig. 1, but for $\sigma = \frac{1}{2}$ and $\tau_1 = 0.39$, $\tau_2 = 202$, and $\tau_3 = 3.5\tau_2$.**

Note that VEV offers the fastest way to deliver a given load but for the price of a larger starting mass due to the large propellant mass. On the other hand, using a maximum propellant velocity gives a strong advantage by reducing the mass of the spacecraft. For comparison, we also show the time-optimized trajectory from Ref. 17, which takes the form adapted to our dimensionless variables:

$$l_{\text{opt}} = \left(\tau^3/3\{[M_0/M(t)] - 1\}\right)^{\frac{1}{2}} \tag{4}$$

Note that, in the time-optimazed scenario, part of the rocket trajectory is described by our more general VEV equations at $\sigma = 1$ (Ref. 17).

It is difficult to evaluate the mass of the tokamak reactor because it is not in the operation yet. Likewise, it is difficult to evaluate the mass of as complex a system as the rocket itself because the technology will evolve by the time the rocket may be built, at least 50 years from now. Initial estimates of the rocket mass and the mass of the fusion reactor produced the specific power $\alpha \simeq 6$ kW/kg with the mass of the rocket $M_w = 10^6$ kg, and the power of the D–He$^3$ fueled reactor $P = 7$ GW, $\eta \simeq 0.85$ (Refs. 7 and 8). Such specific power is consistent with other fusion concepts.[1,9] A large contribution to the mass of the spaceship comes from radiators, which led to the choice of D–He$^3$ as a fuel because D–T plasma produces neutrons. Also, in a D–T reactor, neutrons carry most of the generated power, so that after its transformation to electricity, the heat waste requires a lot (up to one-half) of the power to be radiated, and, thus, the mass of the rocket should increase. On the other hand, at present, D–T is the only type of fuel for experiments on fusion reactors, and moving to D–He$^3$ will meet new challenges in achieving burning conditions. In the following, we will consider both fuels for the fusion reactor, D–T and D–He$^3$.

From Eq. (3), it follows that parameters critical for rocket performance are $\alpha$, $v_{\min}$, and $M_L/M_w$. Parameter $v_{\max}$ does not enter into the normalization constants and affects only how far the rocket can go, that is, when stage three starts, without changing its performance on the first and second stages. In the sense of performance, there is no difference between VEV for D–T and D–He$^3$ if $\alpha$, $v_{\min}$, and $M_L/M_w$ are the same. We apply VEV and CEV to the preceding example from Refs. 7 and 8, in which we substitute the D–He$^3$ fusion birth velocity of protons to the maximum propellant exhaust velocity, $v_{\max} = 5.4 \times 10^9$ cm/s, and we choose $v_{\max}/v_{\min} = 400$. For the minimum velocity, the thermal velocity of the hydrogen plasma used for the propellant with the temperature $T_{\min} = m_H v_{\min}^2/2 = 92$ eV is used. Such a temperature is characteristic for the plasma at the edge of the tokamak, as well as in the Hall thrusters, and seems reasonable to assume for the externally confined plasma outside the tokamak.

It is now easy to find the required flight time using the length

$$\frac{v_{\min}^3 M_0}{2\eta P} = \left(\frac{v_{\min}}{10^7 \text{ cm/s}}\right)^3 \left(1 + \frac{M_L}{M_w}\right) \frac{M_0}{M} \frac{10^9}{2\alpha} \text{ km}$$

$$= 2.25 \times 10^8 \frac{M_0}{M} \text{km}$$

and time

$$\frac{v_{\min}^2 M_0}{2\eta P} = \left(\frac{v_{\min}}{10^7 \text{ cm/s}}\right)^2 \left(1 + \frac{M_L}{M_w}\right) \frac{M_0}{M} \frac{10^7}{2\alpha} \text{ s} = 1.67 \times 10^6 \frac{M_0}{M} \text{ s}$$

normalization constants at $\alpha = 6$ kW/kg, $v_{\min} = 1.35 \times 10^7$ cm/s, and $M_L/M_w = 0.1$.

Dependencies, shown in Fig. 3, correspond to the VEV model with two values of parameter $\sigma = \frac{1}{2}$ and $\frac{1}{5}$ and the conventional CEV model. Corresponding normalized values of $l$ and $\tau$, as well as mass ratios, can be found from Figs. 1 and 2, where the real time curve $t$, years, for chosen normalization constants, is shown. There is always an advantage in time for a given distance of VEV curves dependence over the CEV curve dependence of up to an order of magnitude. In this comparison, we require that the mass in both cases be the same at the destination. The CEV case offers a significant advantage with respect to final mass to starting mass ratio. According to Fig. 3, it will take around one year to reach Pluto, that is, $L = 67$ astronomical units AU $= 10^{10}$ km, and around two months to reach Mars ($L \simeq 2.7$ AU $= 4 \times 10^8$ km). For the extrasolar-system flights, such as Tau missions with $L \simeq 10^3$, it will take around 10 years, which is in agreement with the estimates from

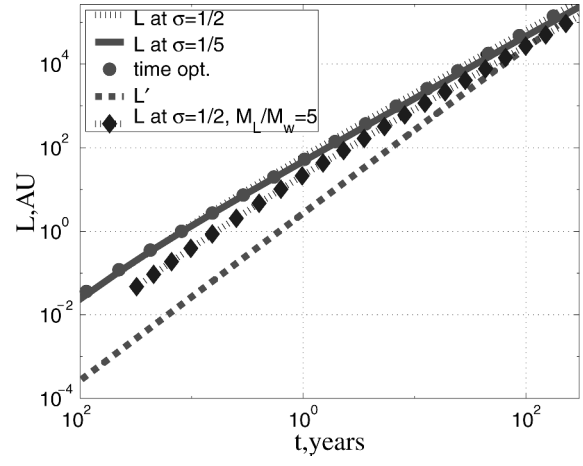


**Fig. 3 Performance of the tokamak thruster rocket shown as dependence of the real distance from the starting point vs time for the space flight according to the modified rocket equation, VEV, and conventional rocket equation, CEV, with the load to thruster mass ratio $M_L/M_w = 0.1$.**

Ref. 9. To show the effect of payload mass on the performance, we draw a VEV flight distance for $M_L/M_w = 5$ in Fig. 3. Shown are the distances $L$, for VEV with $\sigma = \frac{1}{2}$ as a dotted line, $L$ for VEV with $\sigma = \frac{1}{5}$ with time optimized distance from Ref. 17 as circles, and CEV distance $L'$ as a dashed line. For the comparison we provide the VEV distance at $\sigma = \frac{1}{2}$ and mass ratio $M_L/M_w = 5$.

There are many issues in the spaceship design requiring detailed consideration, and these should be considered carefully in separate studies as tokamak machines as reactors become more realistic. One of them is a generic for the issue of heat waste nuclear reactors.[20] This may impose strong restrictions on the performance of the rocket, especially the D–T fueled one. However, we can formulate the requirements of the heat-waste system. In the case of D–T fuel, neutrons would need to be absorbed in the blanket, and then the thermal energy would have to be transformed to electrical energy, which is not typically, efficient. In this case, a considerable fraction of generated power would have to be radiated. Therefore, the prospects of using D–T plasma will depend on the efficiency of the technology of neutron power transformation and the waste-heat radiation. In the case of D–$He^3$ fuel, the main energy loss from the plasma is the thermal flux of the background plasma to the walls, which can be reduced by increasing the energy confinement time. In D–$He^3$ plasma, the thermal flux is determined by

$$P_{\text{loss}} = n_{\text{pl}} T V_{\text{pl}}/\tau_E = (1-\eta) P \tag{5}$$

Here, the second equation follows from the requirement that the plasma is in a self-sustained burning stage, in which the power not used for propulsion is utilized to compensate for losses. The corresponding Lawson criteria for ignition is defined by the critical value of the product $n_{\text{pl}} T \tau_E (1-\eta)$. Requiring it to be fixed, we obtain, from Eq. (5), $P \sim [\tau_E(1-\eta)]^{-2}$. This means that by increasing the confinement time and increasing the effectiveness of the propulsion system, that is, increasing $\eta < 1$ [so that $\tau_E(1-\eta) = \text{const}$] at the same reactor power, we reduce the thermal flux. This is in contrast to the terrestrial tokamak reactors with $\eta = 0$, where an increase in $\tau_E$ leads to the lower power (in burning plasma). The estimate of the plasma energy confinement time requires very careful consideration and experimentation. Note that conditions close to ours are achieved in experiments on the electric tokamak,[21–24] where fast particle ripple losses are used to create a very strong radial electric field and strong plasma rotation. At parameters similar to those in tokamaks, the electric tokamak gives approximately an order of magnitude increase in the confinement time at a smaller magnetic field, for which aluminum toroidal field coils were used. The obtained energy confinement time scalings allowed projections to be be made for reactor conditions[21] and showed that the confinement time may be up to two orders of magnitude higher than in conventional tokamak reactors. Such a significant increase in the confinement time leads to as low as 1% of the generated power contribution to the heat waste from a thermal plasma flux and makes heat waste tolerable in a D–$He^3$ fueled tokamak. Further experiments and extensive diagnostics of particle and energy losses in an electric tokamak are of interest for the fusion plasma thruster concept.

From Fig. 3, it follows that chosen parameters require around 300 years for the trip to the closest star, Proxima Centauri, which is $2.7 \times 10^5$ AU $\sim 0.4 \times 10^{14}$ km away from the Earth. To make such a trip in 50 years, one would have to design a rocket with the generator specific power on the order of $\alpha = 500$ kW/kg. The most advanced, liquid lithium tokamak concept[25] for the reactor allows a much higher-power concentration in the unit than other concepts.[15] The plasma pressure scaling of the power of the reactor can be approximately determined from Eq. (5), $P = n_{\text{pl}} T V_{\text{pl}}/\tau_E(1-\eta) = (n_{\text{pl}}T)^2 V_{\text{pl}}/\tau_E(1-\eta) n_{\text{pl}} T \sim p^2$. In the lithium tokamak, due to the flat temperature profiles, the stability properties of the plasma are significantly improved, and much higher plasma pressure is expected. For a tokamak aspect ratio similar to ITER's, the limit for volume-averaged beta is approximately five times higher, $\beta \equiv 2\mu_0 p/B_\varphi^2 \sim 0.16$, so that the expected power output of an ITER-sized tokamak will increase to $P = 25$ GW. This may improve the specific power, but still will not be enough for the trip to the Proxima Centauri. A further increase in the specific power is possible by constructing a bigger tokamak because the power of the tokamak reactor increases as a volume, that is, $P \sim R_0^3$. On the other hand, the power losses will also increase linearly with the power so that the mass of the radiator, as well as the mass of other supporting systems, should increase accordingly. Thus, the net gain in the specific power may be achieved by increasing the size of the tokamak if future technologies provide effective means of supporting a fusion reactor.

In the preceding estimates, we did not account for the spaceship slowing down a portion of its trajectory and part of the flight when the thrust is used to transfer the rocket to a lower orbit at the destination. This can easily be done using the formulation presented. The change to the obtained, so-called flyby, time of the flight due to such contributions may be a fraction (always less than one-half) of the times just calculated, but are typically smaller. This is because, in our analysis, we fixed the generated power so that during the slowing down phase at the end of the trip, the mass of the ship is smallest and the ship acceleration is largest [see Eq. (2)]. However, if the rocket is to return with no refueling at the destination point, these contributions are close to one half of the one-way flyby flight time (from the Earth to the destination).

Nevertheless, we showed that the solution to the problem of deep space missions using the fusion-powered propulsion proposed has the obvious advantage of using externally confined plasma in the VEV concept. As follows from the preceding analysis, there is a theoretical feasibility for using the fusion tokamak reactor-based spaceship for interplanetary and Tau missions. The critical problem in this concept is the possibility of extracting the directed particle flux from the tokamak.

## IV. Energetic Ion Extraction from the Tokamak Magnetic Configuration via the Magnetic Field Ripple Loss Mechanism

From the preceding section, it is clear that the use of the fusion products alone can not provide required performance for the interplanetary and Tau missions. Thus, to create VEVs with lower exhaust velocity, an externally confined plasma must be included into the design. The key issue for the prospect of using the tokamak as a thruster is a problem of power extraction from the tokamak closed-field-line magnetic configuration, which is investigated in this section in detail. We explore the main properties of such an extraction, define requirements to the magnetic field coils, and show the path to optimize the tokamak configuration. Our idea of using ripple diffusion for fusion propulsion is new. It distinguishes our toroidal fusion concept from other concepts using tokamaks or other fusion devices for the propulsion.

In the toroidal magnetic configurations under consideration, the charged particle is drifting along the axis of symmetry due to the gradient of the toroidal magnetic field. The direction of the drift depends on the sign of the particle charge. In reality, the toroidal magnetic field is not perfectly axisymmetric. Because of the finite distance between the toroidal field coils, the magnetic field has oscillations in the absolute value along the field line, that is, so-called ripples. As a result, without the plasma, the magnetic field is a periodic function of the distance along its line and has the period equal to the distance between the coils.

It is well known that in tokamaks, due to ripples, charged particles can stochastically diffuse in the direction of the drift, get trapped in the magnetic well between the toroidal field coils, and eventually be lost. However, only energetic particles are affected by this mechanism, which may produce both indirect and direct thrust. Stochastic ripple diffusion in tokamaks has a threshold, as shown in Ref. 26:

$$\delta > \delta_{\text{cr}} = \rho_L^{-1} q'^{-1} (\pi N_{\text{coil}} q/\epsilon)^{-\frac{3}{2}}$$

The quantity $\delta$ is typically an exponential function of $r$ increasing rapidly from the center to the edge, so that the effect of ripples is very selective in space. Figure 4 shows a sketch of particle motion when it becomes trapped between the toroidal-field coils. In space, there is no need for the vacuum chamber, so that the tokamak will consist of the magnetic field coils with supporting systems. Once the

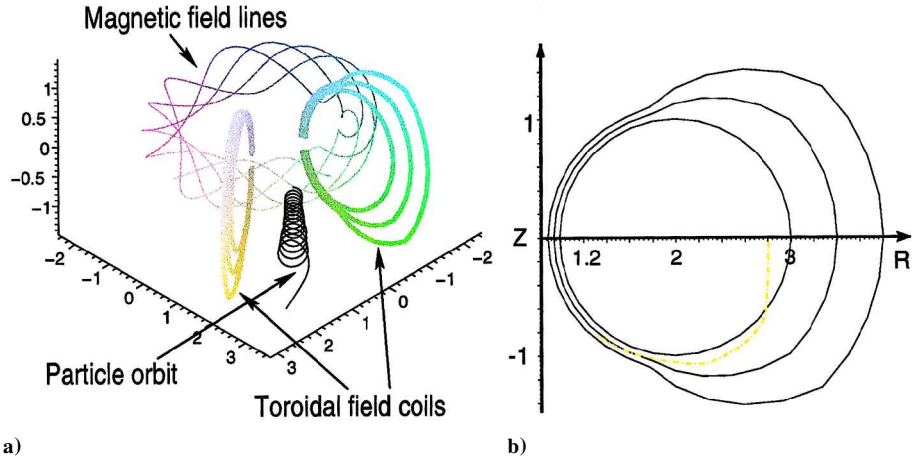


**Fig. 4 Toroidal field coils and the magnetic field lines for one of the configurations studied with major radius $R_0 = 2$, and minor radius $r = 1$: a) two neighboring coils, each consisting of three wires (shown also is the charged particle orbit when it becomes trapped between the toroidal field coils) and b) toroidal coil is shown in its projection to the poloidal plain; – – –, part of the guiding center orbit of a charged particle below the midplane.**

charged energetic particle leaves the tokamak magnetic field closed configuration, it can move freely, except that in our design of VEV the external plasma confined in the outside magnetic "container" will capture such fast particles for subsequent cooling in the low-temperature plasma.

The magnitude of ripples depends on the design of the toroidal field coils, in particular, their size, the number of coils, and the structure of the current distribution in the coils. This dependence can be used for control of the thrust. For this purpose, the toroidal field coils can be designed in such a way that the asymmetric harmonics of the current distribution, responsible for the ripple amplitude, can be controlled independently from the total current in the coils. In addition, the so-called ferritic inserts between the coils may be used for extra control of the ripple losses by making the toroidal magnetic field more axisymmetric.[27]

In the plasma, only trapped particles are affected by this loss mechanism. The amount of the trapped particle population is approximately equal to $\sqrt{(2\epsilon)}$, at $\epsilon \ll 1$, of the total number of particles for isotropic particle distribution. This means that only a fraction of energetic particles, such as charged-fusion products, will be affected. The rest of the energetic particles will contribute to the energy balance of the burning fusion plasma. To create a stronger direct thrust, one can use the ion cyclotron resonance heating (ICRH) of charged particles, the technique widely used in tokamak research.[2] ICRH is efficient in scattering particles from the passing to the trapped domain in the velocity-phase space, where particles will be affected by the ripples. With this process, even background plasma Maxwellian tail ions will be forced to leave the reactor, as was demonstrated experimentally in ICRH plasma discharges in many tokamaks.[28] Ripple losses in tokamak experiments are always localized in toroidal (between the coils) and poloidal (down or up from the midplane) directions. In all tokamak experiments, the toroidal coils are positioned outside the vacuum vessel containing the plasma. A special experiment dedicated to power extraction through the ripple loss mechanism is required.

The power flow for the D–$He^3$ plasma follows. Generated fusion power resides almost completely in the charged fusion products, protons and alphas, $P$. Some fraction of this power needs to be collected and used for the supporting systems and the ICRH, which is needed to scatter passing fast ions to the ripple loss cone. The main power flow goes into the ripple loss cone through fast ions $\eta P$. The rest of the power has to be radiated, $(1-\eta)P$. For the D–T plasma in the case of interplanetary missions, the fusion power is mostly concentrated in neutrons. The challenge for D–T plasma is to collect the neutron power and transform it into electricity, so that it can be used for ICRH of the plasma to scatter alphas and other fast ions into the ripple loss cone, as well as, if required, to transform into other thrusters, such as Hall thrusters. In this case, power used for propulsion is the sum of the power in alphas, $P/5$, and one-half (assume) of the power in neutrons, $\simeq P2/5$. Thus, $\eta \simeq \frac{3}{5}$.

### A. Coil Design Requirements

Once trapped in the toroidal field well, the particle starts to move along the lines of a constant magnetic field with the drift velocity to the zeroth order in $\rho_L/R_0$ (Ref. 29):

$$v_{\rm dr} = \left[\left(v_\parallel^2 + v_\perp^2/2\right)/\omega_c\right]\boldsymbol{b} \times \nabla \ell_n B$$

This means that a single particle having a small Larmor radius can never leave a tokamak magnetic configuration. Plasma particles are trapped on the low-field side of the tokamak, where the ripples are strongest. Then, moving along the $B = \text{const}$ lines, the drifting particle approaches the outer boundary of the toroidal magnetic field coil on the high-field side (HFS) and returns back to the low-field side (LFS). To allow the particle to leave the closed configuration, one needs to exploit the nonconservation of the particle integral of motion (its adiabatic moment), which otherwise provides particle confinement. If coils are designed in such a way that the distance from the particle trajectory to the outer boundary of the coils becomes comparable to the Larmor radius of the particle, it can leave the toroidal configuration. Thus, the coil radial size should be larger than the particle Larmor radius at the LFS $\Delta r_{\rm LFS} \gg \rho_{L0}(1+\epsilon_a)$. The particle moves along the line $B \simeq B_0/(1+\epsilon_a)$. To leave the configuration, it should approach the outer boundary of the HFS part of the toroidal-field coil within a distance smaller than the Larmor radius $\Delta r_{\rm HFS}(1-\epsilon_a)/(1+\epsilon_a) \ll \rho_{L0}(1+\epsilon_a)$, where we assumed that the magnetic field changes linearly across the coil. Thus, the coil should have radial dimensions satisfying the following conditions:

$$\Delta r_{\rm LFS} \gg \rho_{L0}(1+\epsilon_a), \qquad \Delta r_{\rm HFS} \ll \rho_{L0}(1+\epsilon_a)^2/(1-\epsilon_a) \quad (6)$$

Such a coil design meeting these criteria is illustrated in Fig. 4. This coil design will be used in calculations hereafter.

### B. Magnetic Field Model

We developed numerical codes to simulate the energetic particle behavior in the realistic rippled magnetic field of the tokamak. The magnetic field was calculated with a given toroidal coil geometry (Fig. 4) and splined into three-dimensional splines to enhance the numerical performance, so that the resulting magnetic field vector is a function of three spatial coordinates determined by the spline coefficients at the point of interest:

$$\boldsymbol{B} = \boldsymbol{B}(R, Z, \varphi)$$

Such an approach allows the efficient calculation of the vacuum magnetic field for the particle equations of motion.

To describe the equilibrium state of the plasma magnetic field, the high-aspect-ratio approximation ($\epsilon_a \to 0$) with homogeneous current density ($j_0 = \text{const}$) was used.[30] The radial dependence of the magnetic field takes the form

$$B(r) = \begin{cases} CI_0 r/a^2, & 0 \le r \le a \\ CI_0/r, & r > a \end{cases}$$

The equation for the poloidal magnetic flux is given by the solution

$$\psi(r) = \int_0^r 2\pi R B \, \mathrm{d}r$$

keeping equal left and right derivatives at the edge $\psi'_{|r=a}(r \le a) = \psi'_{|r=a}(r \ge a)$. Thus, the expression for the poloidal magnetic flux can be obtained as follows:

$$\psi(r) = \frac{2\pi B_{\varphi a} R_a a^2}{q_a R_0} \begin{cases} \left(\dfrac{r}{a}\right)^2, & 0 \le r \le a \\ \left(1 + 2\,\ell_n \dfrac{r}{a}\right), & r > a \end{cases}$$

Here, to determine the factor $CI_0$, two expressions for the poloidal component of the magnetic field taken at the plasma edge were used:

$$B_\theta(a) = \begin{cases} \dfrac{B_\varphi r}{q(r) R_0} \Big|_{r=a} \\ \dfrac{\psi'}{2\pi R} \Big|_{r=a} \end{cases}$$

Components of magnetic field in spatial coordinates are given by the following formula:

$$B_R = \frac{1}{2\pi R}\frac{\partial \psi}{\partial Z} = \frac{1}{2\pi R}\frac{\partial \psi}{\partial r}\frac{\partial r}{\partial Z}$$

$$B_Z = \frac{-1}{2\pi R}\frac{\partial \psi}{\partial R} = \frac{-1}{2\pi R}\frac{\partial \psi}{\partial r}\frac{\partial r}{\partial R} \tag{7}$$

The variable $r$ is expressed in spatial coordinates by

$$r(R, Z) = \left(8R\left\{3R + R_0 - 4[R^2 - R(R - R_0)/2 - (Z - Z_0)^2/16]^{\frac{1}{2}}\right\}\right)^{\frac{1}{2}}$$

An individual particle obeys the following dimensionless equation of motion:

$$\frac{\mathrm{d}\boldsymbol{v}}{\mathrm{d}t} = \omega_c [\boldsymbol{v} \times \boldsymbol{b}] \tag{8}$$

where we ignored the effects of the plasma on a particle.

To demonstrate the particle extraction in the tokamak, we consider several configurations of the plasma, keeping an edge value of $q$ fixed. We will use dimensionless parameters hereafter. We choose the minor radius $a = 1$ and three major radii $R_0 = 1.2$, 2, and 3. We use 5, 10, or 20 toroidal coils in the examples.

The magnetic field coils are designed to satisfy Eq. (6), as follows. The LFS width is chosen to be 1, whereas the HFS is 0.1. The coil-radial width is slowly changing from the LFS to the HFS. Each coil is represented by three wires, with the first on the outer boundary, the second on the inner boundary, and the third in between. (See Fig. 4 for $R_0 = 2$.)

In calculations, we start with the homogeneous particle distribution over the plasma cross section, so that our estimates will be on the low side of the ion extracting performance. This is because, for example, the particle birth profile is peaked at the center of the plasma. In the numerical run, all particles have one of the Larmor radius to major radius ratios $\rho_L/R_0 = 0.04$, 0.08, 0.16, or 0.32. Particles are also homogeneously distributed over the Larmor rotation phase with six different initial phase angles. The numerical code we developed solves Eq. (8) and follows particle trajectory. Particles are launched toroidally between the coils, which is the most probable result for the particle trajectory after it is trapped in the ripple. The particle pitch angle is taken zero at the starting point $v_\parallel/v = 0$, which corresponds to the bounce point on the particle trajectory.[2] This assumption is not important for the solution to the whole problem in the realistic geometry with the plasma current because a particle changes its pitch angle and process toroidally. When a particle leaves the system, we record its momentum about the vertical axis $p_z$. Each particle can carry a maximum momentum $p_z = 1$. At the end of the numerical run, we calculate the average momentum with which particles are carried away for the given toroidal configuration:

$$P_z = \frac{\sum_j p_{zj}}{N} \tag{9}$$

where $N$ is the number of particles.

### C. Numerical Modeling of Ripple Induced Fast Ion Extraction

Figure 5 shows the comparison of the results for the vacuum toroidal magnetic field and for the configuration with the toroidal plasma current as described in Eq. (7). Particles carry a larger momentum when the plasma current is included (Figs. 5a and 6). The most promising configuration has a moderate aspect ratio with $\epsilon_a = 0.5$ (Fig. 6). The dependence is smoother for this case as a function of Larmor radius, which means that more particles will be contributing to the flux.

The space distribution of the Larmor phase-averaged momentum in the poloidal cross section of the tokamak is shown in Fig. 7. In cases when the plasma current is included, particle losses are distributed over almost all of the poloidal cross section with some fluctuations. This is caused by the numerical errors due to finite numerical accuracy when solving Eq. (8) and by the finite mesh of the particle Larmor gyro phase angle when particles are launched in simulations. Because, in our calculations, we did not specify any

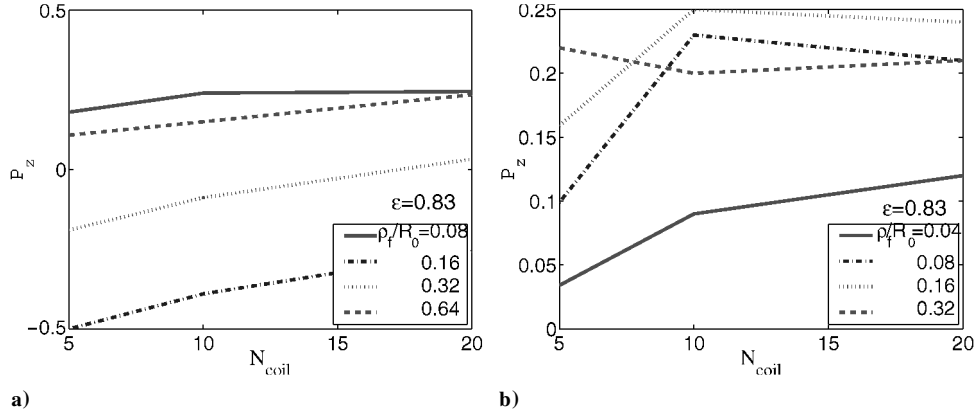


**Fig. 5 Averaged particle vertical momentum depends strongly on the number of toroidal field coils, shown at a fixed inversed aspect ratio $\epsilon_a = 0.83$ for the case with a) no plasma and b) the model equilibrium; Sec. IVB.**

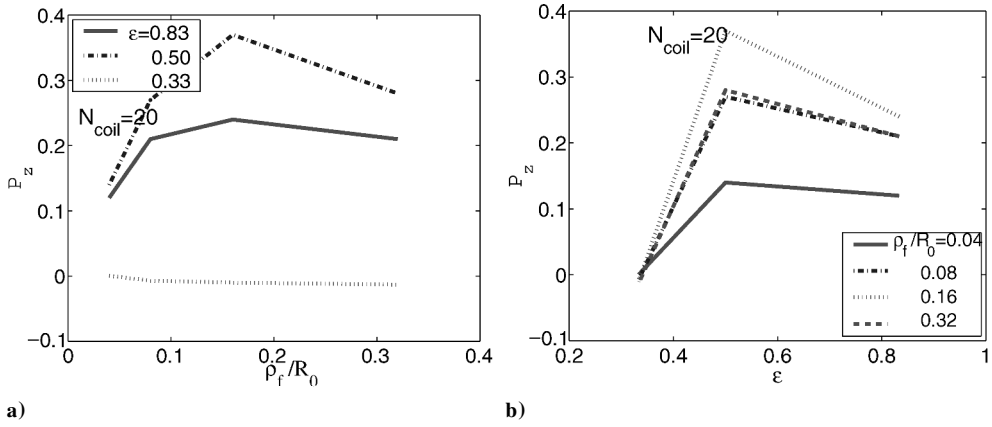


**Fig. 6 Averaged vertical momentum of particles for different aspect ratios and particle Larmor radii presented as functions of a) particle Larmor radius and b) inversed aspect ratio at a fixed number of toroidal coils $N_{\rm coil} = 20$.**

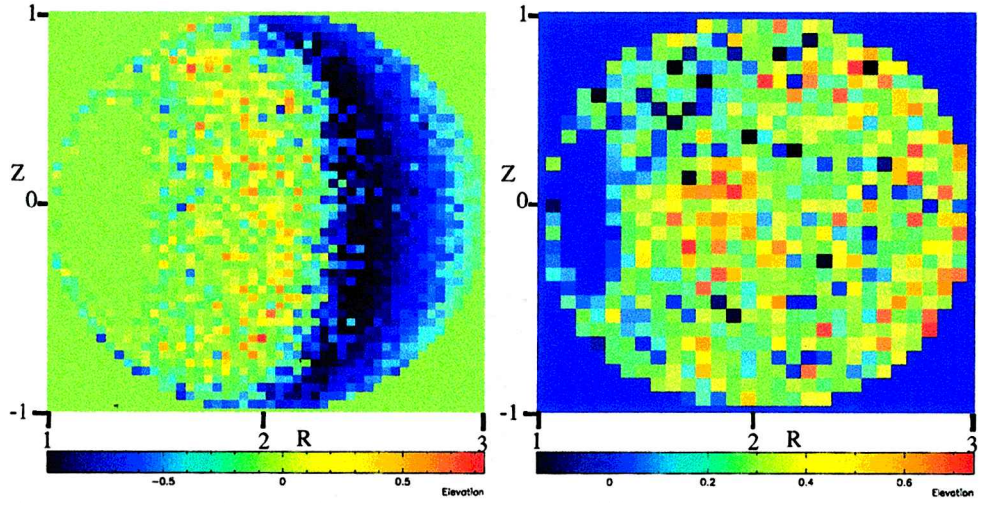


**Fig. 7 Contours of the vertical momentum carried by fusion particles born at a given point in the $R, Z$ plane: a) corresponds to the case when the magnetic field of the plasma is substituted with the vacuum magnetic field and b) corresponds to the plasma with the toroidal current; in these calculations, we had $N_{\rm coil} = 20$, $R_0 = 2$, and $\rho_L/R_0 = 0.08$. [Positive momentum means that particles born at the point $R$, $Z$ contribute to the positive (along the $Z$ axis) vertical momentum.]**

particle birth profile, more realistic profiles can lead to enhanced particle fluxes. However, such an optimization is beyond the scope of this paper.

A very important issue is how particles are distributed in the toroidal angle after they are lost. Figure 8 gives such a distribution for the case $N_{\rm coil} = 20$, $\epsilon_a = 0.5$, and $\rho_L/R_0 = 0.08$. Toroidal field coils are located at the left and right limits of the horizontal axes. The distribution was taken 1 m above or below the coils. This gives some averaging of the distribution in comparison with the one near the coil, but note that the majority of ions are lost between the coils. Some of the particles may collide with the coils, causing damage. A principal solution to this is to set the coils as finite radius wires at those places where particles will most probably impact the coils, as was modeled in the code (Fig. 4). In such cases, a strong magnetic field near the coil will deviate the particles. This imposes an upper limit for the Larmor radius, which can be obtained by restricting the size of the Larmor radius in the vicinity of the coil wire $\rho_{L\rm coil}$ so that it is smaller than the coil radius $\rho_{L\rm coil} < r_{\rm coil}$. With $N_{\rm coil}$ toroidal coils, each consisting of $n$ wires (Fig. 4; $n = 3$), we can write

$$\rho_{L\rm coil} = \rho_L I \sum N_{\rm coil} n r_{\rm coil}/I_{\rm coil} R_0 < r_{\rm coil}$$

or

$$\rho_L/R_0 < 1/N_{\rm coil} n$$

In realistic cases, the allowed Larmor radius is a few times larger than the constraint just obtained, but this is a subject for future studies. Note that the coil wire radius does not meet this criterion because

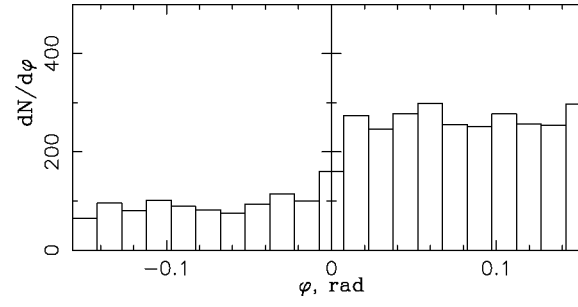


**Fig. 8 Toroidal angle distribution of particle losses for the case with $N_{\rm coil} = 20$, $\epsilon_a = 0.5$, and $\rho_L/R_0 = .08$.**

we assumed that the magnetic field in the vicinity of the coils is due to the wire coil only. This is true if $r_{\rm coil}/R_0 < (1 + \epsilon_a)/Nn$. It follows from here that the concept we are proposing favors rather large devices because $r_{\rm coil} \sim R_0$, and the radius of the coils may be limited by the technology requirements, which are also beyond the scope of this paper.

We have demonstrated numerically that superthermal particles can be extracted from the tokamak with the statistically dominant direction of their velocity. This is the basis for developing the fusion propulsion spaceship powered by a tokamak reactor. We show that by varying such tokamak parameters as the aspect ratio, number of coils, and their shape, the design can be optimized for better power extraction.

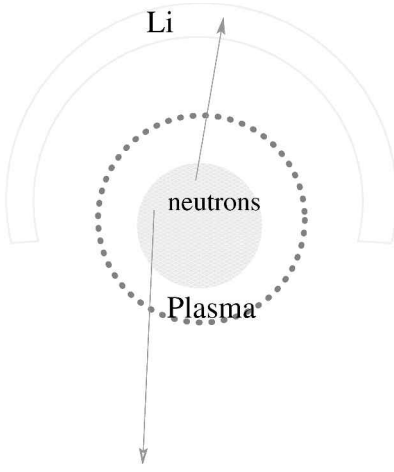


**Fig. 9 Neutron tokamak-based thruster schematic design.**

### D. Direct Neutron Thrust

At present, the D–T fusion reactors are the most realistic for the near future. In this case, fusion 14-MeV neutrons can be utilized for direct thrust. This can be done by placing a blanket, such as liquid lithium, on the upper half of the tokamak reactor as shown schematically in Fig. 9. This blanket has to be placed around the fusion reactor to absorb the energy carried by neutrons. It needs to be at least a few tens of centimeters thick to absorb the neutrons. One-half of the neutrons can be used for such direct thrust, whereas the other one-half will be used for the energy generation and partial tritium recycling. Only part of the particle momentum is used, so that the exhaust velocity of the neutron propellant can be estimated as

$$\langle v_{\|} \rangle \leq v_{n0}/4 = v_{\alpha 0} = 1.3 \times 10^9 \text{ cm/s}$$

Here, we assumed that only positive momentum is carried by the neutrons. This idea is very simple and does not require any special design of the tokamak. Some loss of the efficiency may be associated with the interaction of the neutrons with the coils. Note that this type of propulsion can be used only in interstellar missions due to very low thrust. The serious problem with the neutron type of propulsion is the heat waste, which may impose a constraint on the rocket by increasing its mass.

In the case of a neutron thruster, one-half of the generated power flows directly into the neutrons, $2P/5$. The other one-half of the neutron power, $2P/5$, will be collected and transformed into electricity with subsequent use of ICRH to help scatter the passing alphas into the loss cone. Again, assuming that the efficiency of the heat to electricity conversion is 0.5, we obtain a rough estimate for the power flow to the thrust: $\eta = \frac{4}{5}$.

## V. Summary

We have proposed the concept of a fusion tokamak powered spaceship. This device utilizes advanced physical mechanisms that have not been studied previously. It also has the potential to open up new opportunities for interplanetary and interstellar space exploration.

The proposed solution to the problem of deep space propulsion has obvious advantages because it relies on the controlled VEV concept. Expressions for the VEV rocket dynamic that we obtained can be readily used for development of the concept once the tokamak-reactor design becomes more practical. We show that there is a theoretical feasibility of using the fusion tokamak based spaceship.

Our idea of using ripple diffusion for direct particle extraction from the tokamak is new and distinguishes our toroidal fusion concept from other tokamak concepts or other fusion devices for propulsion. We have demonstrated numerically that superthermal particles can be extracted from the tokamak with the statistically dominant direction of their velocity. This is the basis for developing a fusion propulsion spaceship. Further optimization and more numerical studies are necessary.

New areas of research, both experimental and theoretical, are suggested. In the present-day experiments, the ripple losses are minimized because they contribute to plasma leakage and damage the plasma-facing components. Thus, the use of such a mechanism for thrust creation is a new area of research and needs to be explored in terms of its compatibility with plasma performance. Another area of research is the mechanism of controlling the ripple losses, which translates into the control of the thrust. Both approaches, based on designing the magnetic configuration and affecting the kinetics of the particle losses, should be investigated.

One of the central problems in any concept based on thrust by charged energetic particles is associated with the compensation of their electric charge when they leave the spacecraft. This is a minor issue with the toroidal device. In the absence of the magnetic field outside the spacecraft, any electron gun can resolve it. Inside the plasma and fusion reactor, the static charge may produce the well-known effect of plasma rotation. It also affects the losses of the charged particles and, thus, should be explored in detail.

These studies are closely related to the ongoing plasma confinement experimental and theoretical studies, but have a new focus on handling, rather than minimizing, the particle losses for creating the directed thrust.

## Appendix: Rocket and Rocket-Thrust Equation

For the low-thrust engine, the acceleration should be applied in the direction of the rocket velocity,[19] in which case the gravitational force does not come into the force balance equation, and the rocket equation reads

$$M(t) = M_0 \exp\left( - \int_0^t \frac{\mathrm{d}V/\mathrm{d}t}{v}\, \mathrm{d}t \right) \tag{A1}$$

Consider first the case with CEV $v = \text{const}$. One can obtain from Eq. (A1) the solution in the form of the conventional rocket equation:

$$M(t) = M_0 \exp\{-[V(t) - V_0]/v\} \tag{A2}$$

where $V_0 = V(t = 0)$.

In the case of VEV, generated power can be used most efficiently. For $V = \sigma v$, $\sigma = \text{const} < 1$. By substituting the propellant exhaust velocity in Eq. (A1), we obtain the following modified rocket equation, Eq. (1).

As we argued earlier, to speed up the rocket to the velocity $V_0 = \sigma v_{\max}$, that is, before VEV, we have to use CEV. With Eq. (2), the equation for $u(t)$ is then

$$\frac{\mathrm{d}u}{\mathrm{d}\tau} = e^{u - u_0} \tag{A3}$$

and has a solution

$$u - u_0 = -\ell n[-(\tau - \tau_0) + 1] \tag{A4}$$

which implies that the time required to speed up the rocket to $V_1 = v_{\min}\sigma$ is

$$\tau_1 - \tau_0 = \left[1 - e^{-(u_1 - u_0)}\right] \simeq u_1 = \sigma \tag{A5}$$

On a second stage, we prescribe VEV, that is, $u = \sigma v/v_{\min}$, and make use of Eq. (1) with the substitution $0 \to 1$. Evolution of $u$ is described by

$$\frac{\mathrm{d}u}{\mathrm{d}\tau} = \frac{M_0 \sigma}{M_1 u_1^{\sigma}} u^{\sigma - 1} \tag{A6}$$

and has a solution

$$u = \left[ u_1^{2-\sigma} + \frac{\sigma(2 - \sigma) M_0}{u_1^2 M_1} (\tau - \tau_1) \right]^{1/(2-\sigma)} \tag{A7}$$

It will take

$$\tau_2 - \tau_1 = \left[\left(\frac{u_2}{u_1}\right)^{2-\sigma} - 1\right]\frac{u_1^2 M_1}{\sigma(2-\sigma)M_0} \tag{A8}$$

to accelerate the spaceship up to a speed of $V_2 = \sigma v_{\max}$, which is the limit for the second stage by the definition of VEV, where $v_{\max}$ is the limit velocity for the propellant. Note that in fusion plasma, $v_{\max}$ is equal to the birth velocity of fusion products. Therefore, the third and final stage is again CEV and has to follow Eqs. (A4) and (A5) with the substitution $0 \to 2$ and $1 \to 3$. At stage three, the spaceship will be accelerated until it reaches the designated velocity. Depending on the mission, the ship might reach the required velocity at stage one or two. In the text for shorter notation, we refer to VEV as a notation for the just described combined three-stage scenario CEV–VEV–CEV.

The solution for the whole VEV flight can be written in the form

$$u = \begin{cases} -\ln(-\tau + 1), & \tau < \tau_1 \\ \left[\sigma^{2-\sigma} + \dfrac{(2-\sigma)}{\sigma^{\sigma-1}e^{-\sigma}}(\tau - \tau_1)\right]^{1/(2-\sigma)}, & \tau_1 < \tau < \tau_2 \\ u_2 - \dfrac{v_{\max}}{v_{\min}}\ln\left[(\tau_2 - \tau)\left(\dfrac{v_{\min}}{v_{\max}}\right)^{2-\sigma} + 1\right], & \tau_2 < \tau < \tau_3 \end{cases} \tag{A9}$$

where $\tau_1 = 1 - e^{-\sigma}$, $u_2 = \sigma v_{\max}/v_{\min}$, $\tau_2 = \tau_1 + \sigma e^{-\sigma}(2-\sigma)^{-1}[(v_{\max}/v_{\min})^{2-\sigma} - 1]$, and $u_3$ is the final rocket velocity. The final spaceship mass will be connected with its mass at the start according to

$$M = \begin{cases} M_0 e^{-u}, & \tau < \tau_1 \\ M_0 e^{-\sigma}(\sigma/u)^{\sigma}, & \tau_1 < \tau < \tau_2 \\ M_0 e^{-u v_{\min}/v_{\max}}(v_{\min}/v_{\max})^{\sigma}, & \tau_2 < \tau < \tau_3 \end{cases} \tag{A10}$$

We compare this approach with the conventional rocket equation for CEV, $v = \text{const} = v_{\max}$, in which spaceship velocity is determined by

$$u = -\frac{v_{\max}}{v_{\min}}\ln\left[-\tau\frac{M_0}{M_0'}\left(\frac{v_{\min}}{v_{\max}}\right)^2 + 1\right] \tag{A11}$$

where the prime will refer to the case with CEV, $M_0'$ is the initial mass of the rocket calculated in such a way that at $\tau_3$, the final mass, $M_f = M_w + M_L$, will be the same for both cases, CEV and VEV,

$$M_0' = M_f + \tau_3(v_{\min}/v_{\max})^2 \tag{A12}$$

For a given space mission with a characteristic distance $L$, we can calculate and compare the rocket mass. First, we need to integrate the preceding velocity expressions (A9) and (A11) over $\tau$ to calculate the normalized flight-path time dependence. The result for VEV is

$$l(t) = \begin{cases} (1-\tau)\ln(-\tau + 1) + \tau, & \tau < \tau_1 \\ l(\tau_1) + \dfrac{\sigma^2}{(3-\sigma)e^{\sigma}}\left\{\left[1 + \dfrac{2-\sigma}{\sigma}e^{\sigma}(\tau - \tau_1)\right]^{3-\sigma/2-\sigma} - 1\right\} & \\ \qquad \tau_1 < \tau < \tau_2 & \\ l(\tau_2) + u_2(\tau - \tau_2) + \dfrac{v_{\max}}{v_{\min}} & \\ \quad \times\left\{\tau - \tau_2 + \left[\left(\dfrac{v_{\max}}{v_{\min}}\right)^{2-\sigma} - \tau + \tau_2\right]\right. & \\ \quad \left.\times\ln\left[(\tau_2 - \tau)\left(\dfrac{v_{\min}}{v_{\max}}\right)^{2-\sigma} + 1\right]\right\} & \tau_2 < \tau < \tau_3 \end{cases} \tag{A13}$$

The conventional rocket equation solution, CEV, corresponds to the path evolution:

$$l'(t) = \frac{v_{\max}}{v_{\min}}\left\{\tau + \left[\frac{M_0'}{M_0}\left(\frac{v_{\max}}{v_{\min}}\right)^2 - \tau\right]\ln\left[1 - \tau\frac{M_0}{M_0'}\left(\frac{v_{\min}}{v_{\max}}\right)^2\right]\right\} \tag{A14}$$

## Acknowledgments

We are grateful to S. V. Putvinski, W. J. Emrich, and C. H. Williams for useful discussions. This work was supported in part by U.S. Department of Energy Contract DE-AC02-76CH03073.

## References

[1]Kammash, T. (ed.), *Fusion Energy in Space Propulsion*, Vol. 167, Progress in Astronautics and Aeronautics, AIAA, Washington, DC, 1995, pp. 1–267.

[2]Wesson, J., *Tokamaks*, Clarendon, Oxford, 1997, pp. 1–680.

[3]Peng, M., "The Physics of Spherical Torus Plasmas," *Physics of Plasmas*, Vol. 7, No. 5, 2000, pp. 1681–1692.

[4]Kaye, S. M., Bell, M. G., Bell, R. E., Bialek, J., Bigelow, T., Bitter, M., Bonoli, P., Darrow, D., Efthimion, P., Ferron, J., Fredrickson, E., Gates, D., Grisham, L., Hosea, J., Johnson, D., Kaita, R., Kubota, S., Kugel, H., LeBlanc, B., Maingi, R., Manickam, J., Mau, T. K., Maqueda, R. J., Mazzucato, E., Menard, J., Mueller, D., Nelson, B., Nishino, N., Ono, M., Paoletti, F., Paul, S., Peng, Y.-K. M., Phillips, C. K., Raman, R., Ryan, P., Sabbagh, S. A., Schaffer, M., Skinner, C. H., Stutman, D., Swain, D., Synakowski, E., Takase, Y., Wilgen, J., Wilson, J. R., Zhu, W., Zweben, S., Bers, A., Carter, M., Deng, B., Domier, C., Doyle, E., Finkenthal, M., Hill, K., Jarboe, T., Jardin, S., Ji, H., Lao, L., Lee, K. C., Luhmann, N., Majeski, R., Medley, S., Park, H., Peebles, T., Pinsker, R. I., Porter, G., Ram, A., Rensink, M., Rognlien, T., Stotler, D., Stratton, B., Taylor, G., Wampler, W., Wurden, G. A., Xu, X. Q., and Zeng, L., "Initial Physics Results from the National Spherical Torus Experiment," *Physics of Plasmas*, Vol. 8, No. 5, 2001, pp. 1977–1987.

[5]Sykes, A., Akers, R. J., Appel, L. C., Carolan, P. G., Connor, J. W., Conway, N. J., Counsell, G. F., Dnestrovskij, A., Dnestrovskij, Y. N., Gryaznevich, M., Helander, P., Nightingale, M. P. S., Ribeiro, C., Roach, C. M., Tournianski, M., Walsh, M. J., and Wilson, H. R., *Physical Review Letters*, Vol. 84, No. 3, 2000, p. 495.

[6]Williams, C. H., Borowski, S. K., Dudzinski, L. A., and Juhasz, A. J., "A Spherical Torus Nuclear Fusion Reactor Space Propulsion Vehicle Concept for Fast Interplanetary Piloted and Robotic Missions," *Bulletin of the American Physical Society*, Vol. 44, No. 7, 1999, p. 132.

[7]Borowski, S. K., "A Physics/Engineering Assessment of a Tokamak-Based Magnetic Fusion Rocket," AIAA Paper 86-1759, June 1986.

[8]Borowski, S. K., "Comparison of Fusion/Antiproton Propulsion Systems for Interplanetary Travel," *Fusion Energy in Space Propulsion*, edited by T. Kammash, Vol. 167, Progress in Astronautics and Aeronautics, AIAA, Washington, DC, 1995, pp. 89–127.

[9]Teller, E., Glass, A. J., Fowler, T. K., Hasegawa, A., and Santarius, J. F., "Space Propulsion by Fusion in a Magnetic Dipole," *Fusion Technology*, Vol. 22, 1992, pp. 82–97.

[10]Hooper, E. B., "Plasma Detachment from a Magnetic Nozzle," *Journal of Propulsion and Power*, Vol. 9, No. 3, 1993, pp. 757–763.

[11]Morgan, D. L., "Concepts for the Design of an Antimatter Annihilation Rocket" *Journal of the British Interplanetary Society*, Vol. 35, No. 2, 1982, p. 405.

[12]Ivanov, A. A., Anikeev, A. V., Bagryansky, P. A., Karpushov, A. N., Korepanov, S. A., Kornilov, V. N., Lizunov, A. A., Maximov, V. V., and Murakhtin, S. V., "High Pressure Plasma Confinement and Stability Studies in Gas Dynamic Trap," *Transactions of Fusion Technology*, Vol. 39, No. 1T, 2001, p. 127.

[13]Yatsu, K., Cho, T., Hirata, M., Hojo, H., Ichimura, M., Ishii, K., Itakura, A., Katanuma, I., Kohagura, J., Nakashima, Y., Saita, T., Tamano, T., Tanaka, S., Tatematsu, Y., and Yoshikawa, M., "Progress in High Density Experiments with Potential Confinement on GAMMA-10," *Transactions of Fusion Technology*, Vol. 39, No. 1T, 2001, p. 3.

[14]Emrich, W. J., "End Plugging in the Gasdynamic Mirror Using a Field Reversed Configuration," *Bulletin of the American Physical Society*, Vol. 44, No. 7, 1999, p. 132.

[15]Aymar, R., "ITER-FEAT—The Future International Burning Plasma Experiment—Present Status," *Plasma Physics and Controlled Fusion*, Vol. 42, Supplement 12B, 2000, pp. B385–B396.

[16]Hawryluk, R. J., Batha, S., Blanchard, W., Beer, M., Bell, M. G., Bell, R. E., Berk, H., Bernabei, S., Bitter, M., Breizman, B., Bretz, N. L., Budny, R., Bush, C. E., Callen, J., Camp, R., Cauman, S., Chang, Z., Cheng, C. Z., Darrow, D. S., Dendy, R. O., Dorland, W., Duong, H., Efthimion, P. C., Ernst, D., Fisch, N. J., Fisher, R., Fonck, R. J., Fredrickson, E. D., Fu, G. Y., Furth, H. P., Gorelenkov, N. N., Grek, B., Grisham, L. R., Hammett, G. W., Hanson, G. R., Hawryluk, R. J., Herrmann, H. W., Herrmann, M. C., Hill, K. W., Hogan, J., Hosea, J. C., Houlberg, W. A., Hughes, M., Hulse, R. A., Jassby, D. L., Jobes, F. C., Johnson, D. W., Kaita, R., Kaye, S., Kim, J. S., Kissick, M., Krasilnikov, A. V., Kugel, H., Kumar, A., Leblanc, B., Levinton, F. M., Ludescher, C., McChesney, J., McCune, D. C., McGuire, K. M., Majeski, R. P., Manickam, J., Mansfeld, D. K., Mazzucato, E., Meade, D. M., Medley, S. S., Mika, R., Mikkelsen, D. R., Mirnov, S. V., Mueller, D., Nagy, A., Navratil, G. A., Nazikian, R., Okabayashi, M., Park, H. K., Park, W., Paul, S. F., Pearson, G., Petrov, M. P., Phillips, C. K., Phillips, M., Ramsey, A. T., Redi, M. H., Rewoldt, G., Reznik, S., Roquemore, A. L., Rogers, J., Ruskov, E., Sabbagh, S. A., Sasao, M., Schilling, G., Schivell, J., Schmidt, G. L., Scott, S. D., Semenov, I., Skinner, C. H., Stevenson, T., Strachan, J. D., Stratton, B. C., Stodiek, W., Synakowski, E., Takahashi, H., Tang, W., Taylor, G., Thompson, M. E., Von Goeler, S., Von Halle, A., Walters, R. T., White, R., Wieland, R. M., Williams, M., Wilson, J. R., Wong, K. L., Wurden, G. A., Yamada, M., Yavorski, V., Young, K. M., Zakharov, L., Zarnstor, M. C., and Zweben, S. J., "Results from D–T Experiments on TFTR and Implications for Achieving an Ignited Plasma," *Philosophical Transactions of the Royal Society of London, Series A: Mathematical and Physical Sciences*, Vol. 357, No. 15, 1999, pp. 443–469.

[17]Stuhlinger, E., *Ion Propulsion for Space Flight*, Missile and Space Technology, McGraw–Hill, New York, 1964, pp. 1–373.

[18]Hosny, A. N., *Propulsion Systems*, Univ. of South Carolina Press, Columbia, SC, 1974, pp. 1–551.

[19]Wiesel, W. E., *Spaceflight Dynamics*, McGraw–Hill, New York, 1989, pp. 1–323.

[20]Angelo, J. A., and Buden, D., "Space Nuclear Power," Orbit, Malabar, FL, 1985, pp. 1–286.

[21]Taylor, R. J., "Plasma Confinement in the UCLA Electric Tokamak," *Bulletin of the American Physical Society*, Vol. 46, 2001, p. 247.

[22]Taylor, R. J., Gauvreau, J.-L., Gilmore, M., Gourdain, P.-A., LaFonteese, D. J., and Schmitz, L. W., "Initial Plasmas in the UCLA Electric Tokamak," International Atomic Energy Agency, Paper IAEA-CN-77/EXP1/07, URL: http://www.iaea.org/programmes/ripc/physics/fec2000/html/fec2000.htm.

[23]"Electric Tokamak," URL:http://et.ucla.edu.

[24]Kissick, M. W., Leboeuf, J.-N., Cowley, S. C., Dawson, J. M., Decyk, V. K., Gourdain, P.-A., Gauvreau, J.-L., Pribyl, P. A., Schmitz, L. W., Sydora, R. D., and Tynan, G. R., "Radial Electric Field Required to Suppress Ion Temperature Gradient Modes in the Electric Tokamak," *Physics Plasmas*, Vol. 6, No. 12, 1999, pp. 4722–4727.

[25]Zakharov, L. E., "Magnetic Propulsion of Intense Lithium Streams in a Tokamak Magnetic Field," *Physical Review Letters*, Vol. 90, No. 4, 2003, p. 045001; also URL: http://w3.pppl.gov/~zakharov/.

[26]Goldston, R. J., White, R. B., and Boozer, A. H., "Confinement of High-Energy Trapped Particles in Tokamaks," *Physical Review Letters*, Vol. 47, No. 9, 1981, pp. 647–649.

[27]Kawashima, H., Satoa, M., Tsuzukia, K., et al., "Demonstration of Ripple Reduction by Ferritic Steel Board Insertion in JFT-2M," *Physics Plasmas*, Vol. 41, No. 1, 2001, p. 257.

[28]Zweben, S. J., Darrow, D. S., and Herrmann, H. W., "Measurements of DT Alpha Particle Loss Near the Outer Midplane of TFTR," *Nuclear Fusion*, Vol. 35, No. 12, 1995, pp. 1445–1455.

[29]Morozov, A. I., and Solov'ev, L. S., "Motion of Charged Particles in Electromagnetic Fields," *Reviews of Plasma Physics*, Vol. 2, edited by M. A. Leontovich, Consultants Bureau, New York, 1966, pp. 201–297.

[30]Zakharov, L. E., and Shafranov, V. D., "Equilibrium of Current-Carrying Plasmas in Toroidal Configurations," *Reviews of Plasma Physics*, Vol. 11, Consultants Bureau, New York, 1981, pp. 153–302.

M. Sichel
*Associate Editor*

**Color reproductions courtesy of Princeton Plasma Physics Laboratory.**